

## Is quantitative T2 sensitive to tumor cell infiltration?

T. S. Ali<sup>1</sup>, T. Bjarnason<sup>1</sup>, B. Sun<sup>1</sup>, X. Lun<sup>1</sup>, D. Senger<sup>1,2</sup>, P. Forsyth<sup>1,3</sup>, J. Dunn<sup>1,4</sup>, and J. R. Mitchell<sup>1,3</sup>

<sup>1</sup>University of Calgary, Calgary, Alberta, Canada, <sup>2</sup>Tom Baker Cancer Centre, <sup>3</sup>Southern Alberta Cancer Research Institute, <sup>4</sup>Hotchkiss Brain Institute

**Introduction:** Quantitative analysis of multi-echo T<sub>2</sub> relaxation data (qT<sub>2</sub>) has been used to discern micro-compartmental structures in brain. T<sub>2</sub> distribution histograms derived from multi-exponential analysis demonstrates anatomical composition of brain and can be used to quantify myelin content in MS patients [1], identify water compartments in MS and PKU pathological tissues [2], and to identify multiple tissue-types in rat glioblastoma tumors [3]. The infiltrative nature of cancers in general, and malignant gliomas in particular, poses a major clinical challenge. Recently, brain tumor initiating cells (BTIC) have been identified in brain malignancies and have been hypothesized to represent the cell of origin for these tumors [4]. We analyzed 5 mouse brains in vivo inoculated with BTIC to characterize the changes in T<sub>2</sub> distributions corresponding to different types of pathological regions of heterogeneous tumors, which were then compared with ex vivo histological stains.

**Methods: Subjects:** BTICs established from fresh surgical specimens were injected into the brains of 5 SCID mice [5]. Tumors were allowed to establish and mice were scanned on day 92 followed by immediate sacrifice. The brains were fixed, paraffin embedded, cut into 5 μm thick slices, and prepared for immunohistochemical analysis. Slices within the MR scan were stained with a neural specific progenitor marker (nestin) that can selectively show tumor cell cytoskeleton so that the density of the stain represents tumor cell

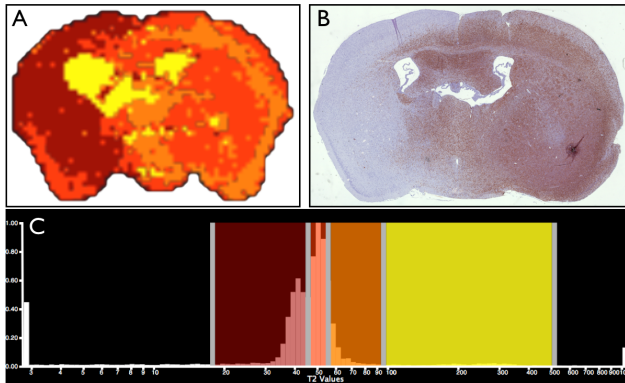


Fig 1: Segmented and color coded gmT<sub>2</sub> map (A), nestin stained histology (B), and color-coded T<sub>2</sub> distribution histogram (C).

population. **MRI Analysis:** Mice were scanned using a single-slice qT<sub>2</sub> acquisition, through the site of BTIC injection, on a 9.4T Bruker console. qT<sub>2</sub> acquisition parameters were as follows: 128 echoes, 5.5ms echo spacing, 3000ms TR, 0.75mm slice thickness, 1.92x1.92cm<sup>2</sup> FOV, matrix 128x128 pixels, 4 averages. After segmenting out the brain, NNLS was performed on a pixel-wise basis [6], creating T<sub>2</sub> distributions for each pixel within the brain. The T<sub>2</sub> times were logarithmically spaced between 2.75 and 1056ms. The decay curves were truncated to 96 echoes from 128 echoes in order to avoid an accumulation artifact. The qT<sub>2</sub> data were visualized and analyzed using in-house software (qT<sub>2</sub>-View), which allows brain to be segmented according to T<sub>2</sub> values specified from the T<sub>2</sub> distribution histogram. For each mouse, 4 T<sub>2</sub> bands (Fig 1C) were defined as follows: 18.39-45.24 ms (normal appearing peak, T<sub>2</sub> band 1, dark red), 47.56-52.56 ms (secondary peak, T<sub>2</sub> band 2, red), 55.25-95.77 ms (shoulder of secondary peak, T<sub>2</sub> band 3, orange), and 100.68-524.35 ms (prolonged peak, T<sub>2</sub> band 4, yellow). For each T<sub>2</sub> band, an area fraction

map and a gmT<sub>2</sub> map were computed. Next, an ROI was drawn on the gmT<sub>2</sub> map including regions highlighted for each T<sub>2</sub> band as shown color-coded in Fig 1A. A local T<sub>2</sub> distribution histogram was created using data only within the ROI. The local histogram was divided up into the 4 T<sub>2</sub> bands described previously and area fractions and gmT<sub>2</sub> times were calculated.

	Area Fraction				Geometric Mean T <sub>2</sub>			
	T <sub>2</sub> Band 1	T <sub>2</sub> Band 2	T <sub>2</sub> Band 3	T <sub>2</sub> Band 4*	T <sub>2</sub> Band 1	T <sub>2</sub> Band 2	T <sub>2</sub> Band 3	T <sub>2</sub> Band 4*
ROI 1	66.8 ± 2.4	14.7 ± 6.0	0.5 ± 0.1	3.0 ± 0.6	38.9 ± 0.3	48.3 ± 0.5	66.1 ± 2.6	272.7 ± 12.0
ROI 2	3.8 ± 0.7	48.7 ± 5.0	11.2 ± 2.1	1.9 ± 0.8	31.9 ± 1.5	50.1 ± 0.6	59.3 ± 0.6	237.4 ± 16.2
ROI 3	2.2 ± 0.8	16.4 ± 3.0	44.0 ± 3.5	1.2 ± 0.3	30.0 ± 1.0	50.8 ± 0.7	60.4 ± 0.8	228.7 ± 18.2
ROI 4	10.6 ± 3.2	30.4 ± 10.4	8.6 ± 3.6	28.4 ± 11.9	38.5 ± 2.5	48.8 ± 0.4	70.3 ± 1.9	293.4 ± 7.0

Table 1: Area fractions and gmT<sub>2</sub> for each T<sub>2</sub> band in 4 ROIs. Standard error shown. \*Only present in 3 mice.

nestin stained histology slice is shown in Fig 1B. Table 1 shows the area fractions and gmT<sub>2</sub> times for the 4 T<sub>2</sub> bands defined for each ROI.

**Discussion:** This study suggests that gmT<sub>2</sub> values lengthen with the presence of tumor cells. The existence of area fractions among different T<sub>2</sub> bands for each ROI demonstrate the multiexponential behaviour due to the heterogeneous nature of the cancer, although the T<sub>2</sub> band defining the ROI predominated the T<sub>2</sub> distribution. The prolonged peak (T<sub>2</sub> band 4), when it was present, had a large intensity peak corresponding to the T<sub>2</sub> band 2. It was only present in 3 mice, which may indicate a specific behavioral pattern of the cancer. Based on the qualitative comparison between segmented gmT<sub>2</sub> maps and histology slides the 4 color-coded regions shown in Fig 1A generated from 4 T<sub>2</sub> bands appear to correspond with varying tumor cell densities in Fig 1B. Through our analysis, we have identified distinct regions with different water compartments within BTIC generated brain tumors. The physiological significance of these distinct regions is not yet known.

**Acknowledgements:** Thanks to Piotr Kozlowski for providing the qT<sub>2</sub> pulse sequence.

**References:** [1] Laule *et al.* NeuroImage 40: 1575-80, 2008 [2] Laule *et al.* JMRI 26: 1117-21, 2007 [3] Dortch *et al.* NMR Biomed 22: 609-618, 2009 [4] Singh *et al.* Cancer Res 63:5821-5828, 2003 [5] Kelly *et al.* Stem Cells 27:1722-1733 [6] Bjarnason *et al.* MRM 2009 (in press)